Eur. Phys. J. B **16**, 447–454 (2000)

THE EUROPEAN PHYSICAL JOURNAL B

EDP Sciences

In situ X-ray diffraction investigation of porous silicon strains induced by the freezing of a confined organic fluid

C. Faivre, D. Bellet[a], and G. Dolino[b]

Laboratoire de Spectrométrie Physique, Université J. Fourier (Grenoble-I)[c], BP 87, 38402 St Martin d'Hères Cedex, France

Received 22 October 1999 and Received in final form 25 March 2000

Abstract. High resolution X-ray diffraction is used to perform an *in situ* measurement of the variations of the lattice parameter of the nanometer size crystallites of porous silicon, induced by the freezing of a confined organic fluid, dodecane. Two p^+ type PS layers of 60 and 70% porosity are investigated, and the variations of their lattice parameter with the temperature (in the range 150-300 K) are measured. The experimental curves are discussed in relation with the results of a previous calorimetric study of the freezing of confined dodecane. We explain the observed strains by the presence of capillary stresses, that appear in the layer due to the formation of internal liquid-vapour meniscus during the freezing process of the confined fluid.

PACS. 61.10.-i X-ray diffraction and scattering – 61.43.Gt Powders, porous materials – 64.70.Dv Solid-liquid transitions

1 Introduction

Since the discovery of the photoluminescence properties of porous silicon (PS) by Canham in 1990 [1], this material has been the subject of many fundamental and applied studies motivated by the perspective of new optoelectronic applications [2]. PS layers, which are produced by an electrochemical etching of single crystal silicon wafers in an ethanoic HF solution, exhibit nanometer size pores with a large internal surface. Furthermore, p-type porous silicon is a unique example of a nanoscale porous material with the structural properties of a nearly perfect single crystal, allowing accurate high-resolution X-ray measurements of the variation of PS strain as a function of external parameter [3].

There is also much interest in the filling of the PS pores by various materials either to obtain new nanomaterial alloys [2] or to perform fundamental studies on materials confined in small size volumes. For example when a fluid is confined in pores with diameter in the nanometer range, the freezing temperature is generally shifted to a lower value [4]. Recently we have investigated the liquid-solid transition of an alkane confined in PS, using differential scanning calorimetry (DSC) [5].

Although often neglected, there is a strain of the porous matrix induced by the molecular interactions with the confined fluid that has been observed in previous dilatometry measurements [6]. The freezing of the confined fluid modifies the interface stress, between the adsorbate and the matrix, leading to a variation of the matrix strain. This effect has been observed by dilatometric measurements in porous silica filled by various liquids, as described in the review paper of Litvan [7].

As PS is a good single crystal, high resolution X-ray diffraction can be performed to measure the strain variations induced by various effects (liquid wetting [8], capillary condensation of an alkane vapour [9], temperature variations of the PS lattice parameter [10]). The aim of the present paper is to present an X-ray diffraction study of the PS strains induced by the freezing of a confined alkane.

In Section 2 of this paper, we describe the experimental set-up and the results of our X-ray measurements. In Section 3, we first recall some results obtained previously in other dilatometric studies of freezing strains and then we discuss our results obtained upon heating and cooling and the origin of the observed thermal hysteresis.

2 X-ray experiments

2.1 Experimental conditions

The porous silicon layers are formed through an electrochemical etching of highly boron doped silicon substrates of (001) orientation, with a resistivity of 10^{-2} Ω cm. These p^+ type samples are anodically etched under dark

[a] *Present address*: Laboratoire Génie Physique et Mécanique des Matériaux, ENSPG-INPG, BP 46, 38402 St Martin d'Hères Cedex, France.

[b] e-mail: `Gerard.Dolino@ujf-grenoble.fr`

[c] CNRS UMR 5588

conditions, in an electrolyte composed of hydrofluoric acid (HF), ethanol and water, with a current density j. For the formation of our PS samples, we used standard etching conditions: the 60% porosity sample is anodized in a (25% HF, 25% water and 50% ethanol) electrolyte with a 180 mA/cm^2 current density for 140 seconds, leading to a 20 μm thick PS layer. To form the 70% porosity PS layer of 5 μm thickness, a current density of 80 mA/cm^2 is applied in an electrolyte composed of 17.5% HF, 32.5% water and 50% ethanol, for 95 seconds. After formation, the PS layers are rinsed in deionised water for five minutes, and then air-dried. In p^+ type samples, the pores have cylindrical shape parallel to $\langle 001 \rangle$ directions with a diameter around 10 nm [2].

The X-ray diffraction set-up is a double crystal diffractometer, using a molybdenum source ($\lambda = 0.707$ Å), built for the *in situ* measurement of PS thermal expansion at low temperature [10]. The (004) rocking curve of the sample is obtained by a variation of the sample angle ω, with a detector slit (of 5 mm width) at a fixed position. As the monochromator and the sample are similar (001) silicon wafers, the rocking curve is independent of the beam divergence [11]. To measure very narrow Bragg peaks, we use a motorised screw (with a step of 0.1 μm) acting on a lever of 300 mm, giving a rotation step $\delta\omega = 1.91 \times 10^{-5}$ degree (≈ 0.07 arcsec), which is a better angular resolution than in a previous experiment using a commercial apparatus [9].

A diffraction cell, set on the diffractometer, allows a control of the temperature, in the range of 90 to 300 K, and of the vapour pressure of the adsorbed fluid, from vacuum to the saturation vapour pressure P_s. The vacuum in the cell is produced by a zeolite pump, which prevents any oil pollution. The alkane (dodecane in the present experiment) is introduced in the nanometer pores of PS by small step increase of the vapour pressure, until complete filling. This is obtained when the PS Bragg peak has shifted to a lower angle (*i.e.* to a larger lattice parameter) and has become narrow again, proving that the pores are filled with the liquid [9]. It is sometimes necessary to increase the vapour pressure above P_s to fill completely the nanometer pores [9]; this is performed by slightly heating the liquid reservoir, and/or slightly cooling the cell. There could be an excess liquid film on the external surface of the PS layer but we are not able to check its presence. Indeed, the thickness of this layer is too small to be detected through the decrease of the X-ray intensity, as its absorption is negligible for Mo radiation.

The sample is cooled by liquid nitrogen flow and heated by means of an electrical resistance, while a temperature sensor under the heating and freezing stage allows to control the temperature variations. A small temperature gradient of a few degrees is present in the cell. At low temperature ($T < 200$ K), the actual sample temperature is about 5 K higher than the indicated temperature (which is used below). The X-ray measurements are performed during cooling-heating cycles, with temperature steps every 5 to 20 degrees, each step being reached at a rate of 10 K/min. For each temperature step, a waiting time of 20 to 40 minutes is used to stabilise the temperature in the whole cell, before recording the rocking curves.

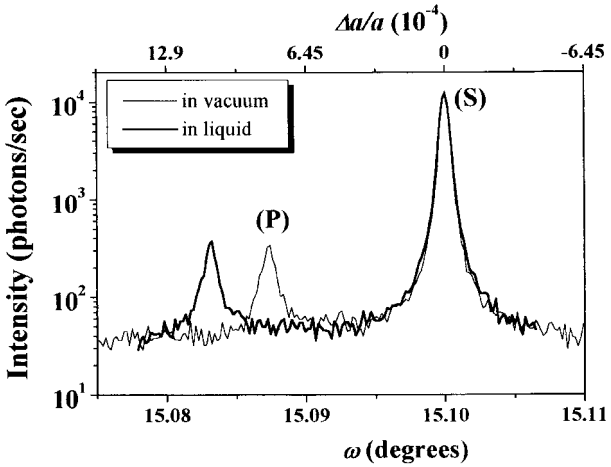

Fig. 1. X-ray rocking curve of the (004) reflection for a p^+ type PS layer of 70% porosity and of 5 μm thickness, in vacuum (_____) and filled by dodecane (_____). (S) and (P) corresponds respectively to the Bragg peaks of the substrate and of the porous layer. (In the rocking curve figures, a log scale is used for the intensity; the ω angular scale is given on the bottom X-axis and the corresponding variations of $\Delta a/a$ are given on the top X-axis.)

The PS sample being vertical, a delicate problem concerns its fixation in the cell. Indeed, due to the large temperature range of this experiment, a classical fixation using glue or small metallic clips induces an important curvature of the sample as the temperature decreases. The problem is solved by introducing a small magnet in the back of the cell with two small iron strips placed on the non-porous edges of the PS sample, holding the vertical sample with very weak induced strains.

2.2 Experimental results

The rocking curves of the (004) reflection are shown in Figure 1 for a p^+ type PS layer of 70% porosity and 5 μm thickness, measured first in vacuum and after a complete filling with dodecane. As usual for PS samples, the rocking curve exhibits two Bragg peaks: (S) corresponds to the diffraction of the silicon substrate and (P) of the PS layer, which has a slightly different lattice parameter [12]. For the sample in vacuum, the relative mismatch between the PS lattice parameter and that of the silicon substrate is $\Delta a/a = 8.2 \times 10^{-4}$. The full width at half maximum (FWHM) of the substrate peak is 2 arcsec while the theoretical value in the same conditions is 1.3 arcsec; the PS Bragg peak is a little broader with a FWHM of 3.5 arcsec, showing the good crystalline properties of the porous silicon layer. For the sample fully filled with dodecane, one clearly sees the shift of the PS Bragg peak to a lower diffraction angle, showing an increase of the lattice parameter to $\Delta a/a = 10.8 \times 10^{-4}$, as observed previously [8].

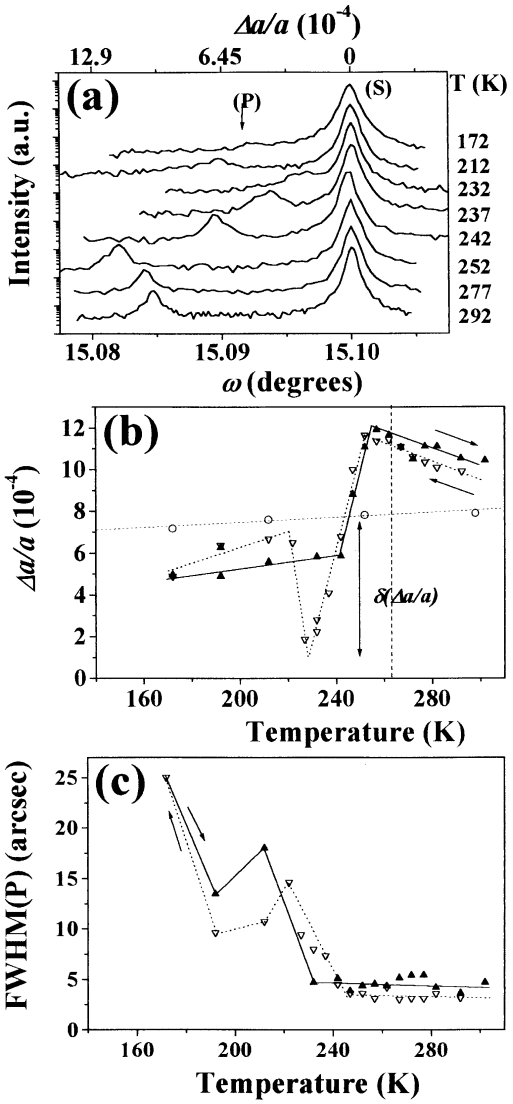

Fig. 2. Strain variations as a function of temperature for a p^+ type PS layer of 70% porosity and 5 μm thickness filled with dodecane. (a) Rocking curves of the (004) reflection, measured at various temperatures upon cooling. The rocking curves have been aligned on the position of the substrate Bragg peak at room temperature and have been shifted vertically on the logarithmic intensity scale. (b) The lattice mismatch parameter ($\Delta a/a$), is plotted as a function of temperature, for a dry PS layer in vacuum (○) and for a PS layer filled by dodecane, during a decreasing (▽) and increasing (▲) temperature cycle. The vertical dashed line at 263 K corresponds to the freezing temperature of bulk dodecane. (c) Temperature variation of the FWHM of the PS Bragg peak, upon cooling (▽) and upon heating (▲). The lines are only a guide for the eye, and the arrows indicate the temperature variation directions.

The temperature variations of the rocking curves of the PS sample of 70% porosity, filled with dodecane, are plotted in Figure 2a. In this experiment the temperature T was changed from $T = 292$ K to $T = 172$ K and for each temperature step, rocking curves were recorded, that allow to measure the lattice mismatch parameter $\Delta a/a$ and of the PS Bragg peak FWHM plotted respectively in Figures 2b and 2c. In successive temperature cycles performed under the same conditions, similar results were obtained. The thermal expansion of the dry sample measured in vacuum [10] is also plotted in Figure 2b.

In Figure 2, the displacement and the broadening of the PS Bragg peaks with temperature are clearly exhibited as the temperature decreases. The first diffraction profile, recorded at $T = 292$ K corresponds to a PS layer filled by liquid dodecane while the last profile, recorded at $T = 172$ K, corresponds to the sample filled by solid dodecane. Indeed our calorimetric measurements [5], have shown that dodecane confined in a similar p^+ type PS layer (with a pore diameter around 7 nm) is frozen below 230 K. Three temperature ranges can be distinguished in the variations of $\Delta a/a$ and of the FWHM:

- From $T = 292$ K to 252 K, the PS layer lattice parameter increases with no visible broadening of the PS Bragg peak (FWHM ≈ 3.5 arcsec), indicating that the strains are homogeneous, when the pores are filled by liquid dodecane. There is no anomalous variation around the freezing temperature of bulk dodecane at $T_{\text{bulk}} = 263$ K.
- Between $T = 252$ K and $T = 220$ K, freezing occurs. First $\Delta a/a$ decreases drastically from 12×10^{-4} at $T = 252$ K to about 2×10^{-4} around $T = 230$ K. The $\Delta a/a$ variation is surprisingly linear as a function of temperature and the slope is fifty times larger than the thermal expansion of the same sample in vacuum. For lower temperatures, $\Delta a/a$ increases again reaching a maximum value of 6.5×10^{-4} around $T = 220$ K. A broadening of the PS Bragg peak is observed below $T = 237$ K, with a maximum value of the FWHM of 14 arcsec at $T = 220$ K.
- Below $T = 220$ K, the pores are probably filled by solid dodecane and $\Delta a/a$ decreases linearly with temperature, while the FWHM first decreases to about 10 arcsec. For the last measurement at $T = 172$ K, the PS Bragg peak has shifted to a diffraction angle (indicated by an arrow in Fig. 2a) corresponding to $\Delta a/a = 4.7 \times 10^{-4}$. The PS Bragg peak is broader, reaching a FWHM = 25 arcsec. At a lower $T = 152$ K, the PS Bragg peak is too broad to be observed and therefore it is no more possible to determine $\Delta a/a$.

Upon heating, the lattice mismatch parameter first increases with the temperature as in the low temperature part of the cooling curve, but with a slightly smaller slope; the FWHM decreases to a smaller value, about 5 arcsec, around $T = 232$ K. There is no important variation of $\Delta a/a$ in the temperature region where a dip was present upon cooling. A sharp increase of $\Delta a/a$ starts only at $T = 242$ K, which can be considered as the beginning of the melting. Then upon heating the data points follow the same curve as upon cooling, but with an upward temperature shift of 2 to 3 K, which however is close to the temperature incertitude. For T increasing above 255 K, there is again a slow decrease of $\Delta a/a$ corresponding to a PS layer filled by liquid dodecane (the small upward temperature shift of $\Delta a/a$ relative to the initial cooling,

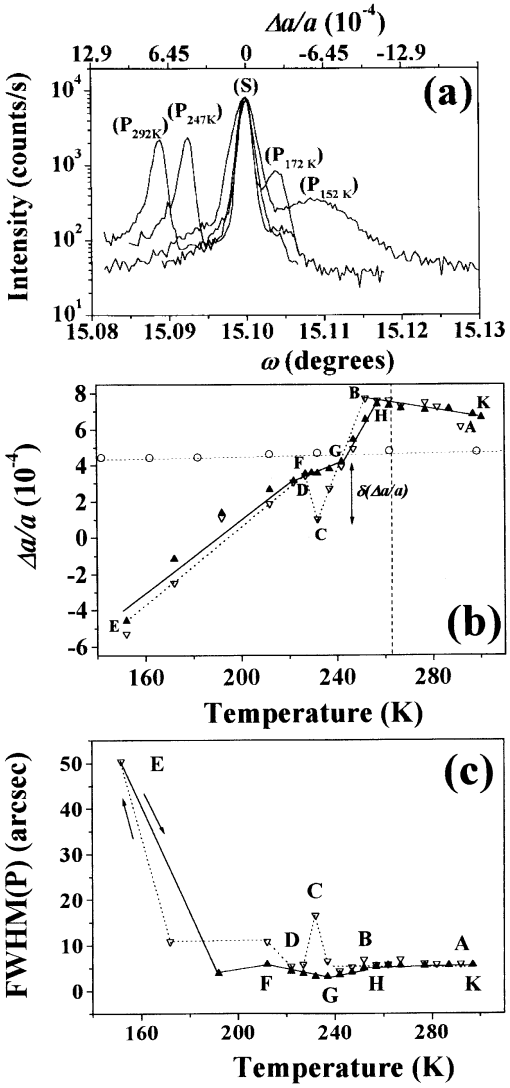

Fig. 3. Strain variations as a function of temperature for a p^+ type PS layer of 60% porosity and 20 μm thickness with dodecane (with the same presentation as in Fig. 2). (a) Rocking curves around the (004) reflection, measured at various temperatures upon cooling. (b) Lattice mismatch parameter ($\Delta a/a$), plotted as a function of the temperature for the p^+ type PS layer of 60% porosity in vacuum (○) and for a layer filled by dodecane, during a decreasing (▽) and increasing (▲) temperature cycle. (c) Temperature variation of the FWHM of the PS Bragg peak, upon cooling (▽) and upon heating (▲).

observed in Figure 2b, is probably due a small modification of the surface stress, during the long duration (30 h) of the measurement).

In Figure 3, we report the results of the same experiment performed on another PS sample, with a smaller porosity of 60%. In Figure 3a are shown some of the diffraction profiles recorded during the cooling scan from $T = 292$ to 152 K. The variations of $\Delta a/a$ and of the FWHM are presented respectively in Figures 3b and 3c. For the cooling curve, starting at $T = 292$ K, the lattice mismatch parameter $\Delta a/a = 6 \times 10^{-4}$ increases slightly

Table 1. Freezing and melting temperatures of dodecane confined in a p^+ type PS layer of 60% porosity, obtained from the DSC results of reference [5] and from the X-ray strain data of Figure 3b. For the DSC peaks, $T_{\rm low}$, T^* and $T_{\rm high}$ are respectively the temperature of the lower limit, of the maximum value and of the higher limit of the DSC peaks, observed upon cooling and upon heating; for the X-ray results of Figure 3b, the temperatures are those of points B, C, D upon cooling and G and H upon heating.

	Measurement	$T_{\rm low}$(K)	T^*(K)	$T_{\rm high}$(K)
Freezing	DSC	235	243	253
	X-ray	(D) 227	(C) 232	(B) 252
Melting	DSC	235	254	260
	X-ray	(G) 242		(H) 257

for decreasing T. Below $T = 252$ K, $\Delta a/a$ drastically decreases to reach a minimum value around 1×10^{-4}, for $T = 232$ K. At this temperature, the PS layer diffraction peak is broader, with a FWHM $\approx$ 14 arcsec. Then for a lower temperature of $T = 227$ K, $\Delta a/a$ increases to 3×10^{-4} and the PS peak is again narrower, showing the end of the transition region: the confined dodecane is completely in the solid phase. For a further decrease of the temperature, the PS Bragg peak shifts to larger angles, crossing the substrate peak around $T \approx 200$ K, where $\Delta a/a = 0$. For the lower measurement temperature ($T = 152$ K), the PS lattice parameter is smaller than the lattice parameter of bulk silicon, leading to a negative value of $\Delta a/a = -5.3 \times 10^{-4}$; the PS Bragg peak is again rather broad with a FWHM $\approx$ 50 arcsec, revealing the presence of inhomogeneous strains in the porous layer.

Upon heating, the behaviour of $\Delta a/a$ is very similar to that of the first sample, showing no dip in the melting region, while the FWHM as already reached a constant minimum value at 192 K. The temperatures of the various transition features observed upon cooling and heating for the 60% porosity sample are collected in Table 1 and will be used in the following discussion.

The main differences between the two PS layers come from the variation of the porosity values. The 60% porosity sample has a smaller strain at room temperature while its average elastic constants are larger [13], which leads to more homogeneous deformations. It is then possible to follow the PS Bragg peak to lower temperatures than in the case of the 70% porosity sample.

3 Discussion

3.1 Freezing strains due to confined fluids

According to the classical work of Defay and Prigogine [4], the physical properties of small size materials are modified by the contribution of surface properties. Since in

our previous work [5] we have critically reviewed the thermodynamic basis of phase transitions of confined liquids, in the present paper we give only a brief introduction to this subject, where we emphasise the few publications reporting measurements of the freezing strains.

For a fluid confined in nanometer size pores, there is an extension of the existence range of the liquid phase in the temperature-pressure phase diagram:

- The vapour-liquid transition is most often observed during an isothermal variation of the pressure. Capillary condensation of the liquid phase in the pores occurs at a pressure lower than the bulk saturation vapour pressure. Then the Kelvin equation, which gives a relation between the capillary condensation pressure and the curvature of the liquid-vapour interface, allows a determination of pore radius [14]. This classical method has been used by Hérino *et al.* to determine the pore radius of various kinds of PS structures [15].
- The liquid-solid transition of a confined liquid occurs generally at a temperature lower than that of the bulk transition. Since, according to Gibbs-Thomson equation, the shift of the transition temperature is proportional to the inverse of the pore radius, this effect can also be used to determine pore size [16]. We have recently used this method to measure PS pore size and its variations during chemical dissolution [5].

In the usual adsorption models, the porous matrix is considered as perfectly rigid, but in fact it is slightly strained by the molecular interactions with the adsorbate, an effect first observed in 1927 by Meehan [17] in charcoal. As described in the review of Sereda and Feldman [6], adsorption strains have been systematically observed in dilatometric measurements of porous materials during isothermal pressure variations. In fact there are two opposite strain effects: the first one is an expansion associated to the decrease of the matrix surface energy due to vapour adsorption. The second one is a contraction, observed during capillary condensation; it is attributed to the large negative pressure produced in the confined liquid by the presence of a concave liquid-vapour meniscus. Larger contraction is observed during desorption than during adsorption.

Freezing of the confined liquids also induces strains in the porous matrix, which have been observed in several dilatometric measurements [18–22] and discussed in the review of Litvan [7]. Most of these studies have been performed on the freezing of water confined in small pores, a phenomenon occurring frequently in nature [23]. Some important results were already obtained in the earlier measurements of Hodgson and McIntosh [18]: a gradual expansion of the matrix was observed during the freezing of water confined in porous silica, a result which is expected for water which expands upon freezing. However a similar expansion was also observed for benzene, a normal liquid which contracts upon freezing. Litvan and McIntosh [19] observed that the two first interfacial liquid monolayers never freeze. Antoniou [20] performed simultaneous calorimetric and dilatometric measurements, which give a good correlation between the two phenomena. However, for unknown reasons, he obtained different results on two similar samples: in one sample the expansion curve shows a dip upon freezing and no dip upon melting as in our results, while in another sample there was dips both upon freezing and melting. Two models have been mostly used to explain the origin of freezing strains induced by confined liquids, but without clear conclusion [18]:

- The first model is a development of the solid meniscus model of Everett [24], which considers the motion of a solid-liquid interface trough pore apertures.
- The second model is based on the transfer of the supercooled liquid from small pores to larger voids or to the external surface, where free bulk crystallisation occurs.

In a very detailed study, Feldman [21] showed that, at least for water freezing, these two effects contribute. For a porous glass saturated of water at room temperature, the initial freezing in the larger pores produces an increase of the adsorbate volume and then the excess liquid is drained out of the pores and crystallised on the external sample surface, as shown by direct visual observations. The contraction of the porous matrix is attributed to the existence of solid meniscus. Although Feldman observed the presence of ice on the external sample surface, there was no evidence of the bulk phase transition in his dilatometry measurements. Furthermore, using a porous sample saturated with water at low temperature, he started his measurements with a heating scan, and then he observed a decrease of the sample length. As the volume of H_2O adsorbate decreases upon melting, the liquid menisci of the adsorbate recede into the pores during melting.

On the other hand, Litvan [22] observed two transitions during the cooling of a porous glass saturated with water: around 266 K, there was a large thermal perturbation, corresponding to the freezing of an external water layer, while the gradual freezing of water confined in the small pores began around 250 K. The effect of internal meniscus was rejected, the change of length being associated mostly with the decrease of the adsorbate mass inside the pores.

Finally Enüstün *et al.* [25], using volumetric mercury measurements, determine the total volume increase of a porous sample filled by water. They observed only a small volume increase, corresponding to the out draining of the excess water resulting from the expansion of the adsorbate upon freezing. They also report that the strain from external freezing is observed only after a HF etching of the porous glass. For freezing, Enüstün *et al.* favour the interface motion model, which we have also adopted in our previous work [5].

In conclusion the freezing of a confined fluid produces rather large strain in the porous matrix. However the variations observed in previous experiments show that there is some effect which is not well-controlled, as for example the liquid transfer between the pores and the external environment. This effect depends probably on

temperature gradients in the cell and on the rate of temperature variations.

3.2 Interpretation of our freezing and melting results

In order to explain the origin of the strains induced by dodecane freezing in PS, we propose the following model for the three temperature ranges experimentally observed; Figure 3 is commented following closely the arguments of Feldman, using the same letter labels as in his dilatometric measurement [21]:

(i) In the range (AB), for temperature higher than the freezing temperature of confined dodecane, $\Delta a/a$ increases slightly when the temperature is decreased. This effect which is reversible, can be attributed to the temperature variation of the surface stress of the silicon crystallites wetted by liquid dodecane.

(ii) In the freezing range (BD), $\Delta a/a$ decreases first linearly (BC) and then increases again (CD). Dodecane is a normal liquid, which contracts upon freezing: for bulk material, $\Delta V/V \approx -15\%$ for a transition temperature $T_{\rm bulk} = 263$ K. When freezing begins in the largest pores, the adsorbate volume decreases and then a part of pore volume is filled only by vapour. Concave liquid-vapour menisci are then formed, inducing large negative pressure in a part of the confined liquid and inhomogeneous strains in the porous matrix. As noted by Feldman [21], the freezing curves is similar to the curve of the desorption isotherms around the critical pressure. At the end of freezing at point (D), all dodecane is solid and the liquid menisci disappear. The capillary stresses of the liquid menisci are suppressed, leading to an increase of the porous layer lattice parameter at the end of the freezing temperature range.

(iii) In the low temperature range (DE), where all dodecane is frozen in the porous sample, some pores are filled with solid while others filled by vapour are nearly empty. Solid-vapour menisci are then present, producing some stress on the dodecane crystallites, which are elastically and plastically deformed. It is rather difficult to evaluate the strain state of the adsorbate and even more of the adsorbent as interfacial crevices can be present. We can only mention that after freezing there is an average contraction of the porous matrix that may be induced by the contraction of solid dodecane. Upon cooling, a linear decrease of $\Delta a/a$ is observed which mostly comes from the differential thermal expansion between solid dodecane and porous silicon. The strains can become very large since for temperature below $T \approx 200$ K it induces a negative value of $\Delta a/a$ for the 60% porosity PS layer. On the other hand, the strain in the partially empty pores (*i.e.* filled only by dodecane vapour) is only due to the thermal expansion of porous silicon in presence of the vapour. These inhomogeneous stresses produce a large broadening of the Bragg peak of the PS layer that increases with a further decrease of the temperature. In the softer 70% sample, these strains are so large that the narrow coherent Bragg peak cannot be observed below $T = 172$ K. These observations are quite similar to the result obtained on anodically oxidised PS [26] but in the present experiment, the matrix deformations are completely reversible and the PS peak reappears during heating. The observation of these large inhomogeneous stress at low temperature, after freezing of the adsorbate, is a new feature which can only be observed by *in situ* X-ray strain measurements.

Upon heating the 60% sample in the low temperature range (EF), the $\Delta a/a$ variation is reversible from E to F. The major difference between heating and cooling is the absence of a dip in the range (FG). Upon heating the only clear variation occurs at point G, (where starts the drastic increase of $\Delta a/a$), which is tentatively identified with the beginning of the melting. A small hysteresis is observed in the range (GH). Similar behaviours have been observed previously by Antoniou [20] and Feldman [21] for confined water. We recall the analogy of Feldman with the behaviour observed during adsorption and desorption, but there is no precise explanation for the smaller effect observed during melting than during freezing. Furthermore in several cases, dips have also been observed during ice melting [20,22]. Finally in the range (HK) where all dodecane is liquid after the completion of the transition, there is the same linear variation than upon cooling.

We now give a rough evaluation of freezing strain attributed to vapour-liquid menisci in the pores. The maximum variation of $\Delta a/a$ upon freezing (noted $\delta(\Delta a/a)$ in Fig. 2b) results from the negative pressure σ, due to the concave meniscus present in a pore of radius r, given by Laplace equation,

$$\sigma = -\frac{2\gamma_{\rm l\nu}}{r} \tag{1}$$

where $\gamma_{\rm l\nu}$ is the liquid surface tension. For dodecane (with $\gamma_{\rm l\nu} = 25$ mJ/m^2) in pores of radius $r \approx 3.5$ nm, we have $\sigma = -14$ MPa. In a previous work [9], we have given a rough evaluation of the effect of this capillary pressure on PS strains ε, given by

$$\varepsilon = \delta\left(\frac{\Delta a}{a}\right) = \frac{\sigma(1-2\nu)}{E_{\rm p}} \tag{2}$$

where $\nu \approx 0.1$ is the Poisson coefficient for PS [12], $E_{\rm p}$ is the macroscopic Young modulus of the PS layer, which can be expressed as a function of the Young modulus of bulk silicon ($E_{\rm Si} = 166$ GPa) and of the sample porosity P, by $E_{\rm p} = E_{\rm Si}(1-P)^2$ [13]. Then for the 70% porosity PS layer, $\delta(\Delta a/a) \approx 8 \times 10^{-4}$, which is closer to the experimental value (7×10^{-4}) than can be expected from this rough estimation. In the same way, for the 60% p$^+$ type PS layer the estimated value is 4.3×10^{-4}, while the experimental value is 3×10^{-4}.

To discuss the thermal hysteresis observed in Figures 2 and 3, we recall in Table 1 some results of our previous DSC study of the thermal behaviour of dodecane confined in a p$^+$ type PS layer of 60% porosity and 100 μm thickness [5]: the freezing transitions observed in calorimetry and X-ray measurements occur in similar temperature ranges (the agreement is slightly better if we take into account the presence of a small temperature gradient in the cell: in the freezing range the temperature of the sample is

about 5 K larger than the value given by the temperature sensor). However the temperatures T^* of the DSC peak maximum and of the strain dip are rather different: this shows that the strain effect is more sensitive to the spatial distribution of the solid and liquid phases while the thermal signal depends only on the variation of matter between the two phases. For the heating curve in the X-ray measurement, melting occurs between point G and H.

In our previous DSC work were a liquid drop was poured on the PS sample [5], the fluid was clearly in excess on the external surface, and bulk liquid became solid first outside. Then the freezing in PS pores occurred at lower temperatures, with the motion through the pore apertures of the solid-liquid interface (which locally is approximately spherical). In the present experiment we cannot be sure whether some bulk dodecane is or is not present at the external surface, since a thin layer of a few μm on the surface cannot be detected in the present X-ray experiment. If an external solid crust is not present to initiate freezing, then it has to nucleate in the larger pores or in surface crevices. The fact that the transition temperatures are similar in DSC and in the present X-ray experiments, shows that there is no real problem for the nucleation of a solid phase in a PS sample. For melting, the transition mechanism is very different: in principle, the liquid phase must be nucleated in the smallest pores. However the first adsorbate interfacial layers are probably not crystallised and a liquid phase can be easily nucleated in this non-freezing layers, producing eventually a cylindrical liquid layer around a solid core. This model can explain the thermal hysteresis [5] but it is not clear why transition strains are reduced upon heating.

Due to the large strains induced by capillary stresses in high porosity PS [9], the drying of such samples is a delicate step in the fabrication of PS layers. Therefore several studies have been devoted to the drying process of PS, trying to avoid the creation of liquid-vapour interfaces (present in the most common drying method by evaporation) [27]. It was recently shown that an efficient technique to dry high porosity PS layers is freeze-drying [28]: the fluid present inside the pore network is frozen and then sublimed under vacuum. It is somewhat surprising that such a method is so efficient since, at least for dodecane, we have evidenced the presence of capillary stresses during the freezing of the confined fluid, producing strains as large as during evaporation. The relations between freeze-drying and the thermodynamic behaviour of the freezing of confined fluids have been further discussed by Scherer [29]. The next step in the study of freeze-drying of PS, would be to perform X-ray measurements during the freezing of water confined in PS. This experiment would be quite interesting, since contrary to most organic materials, water expands upon freezing.

4 Conclusion

Using high-resolution X-ray diffraction, we have measured the strains induced by the freezing of an organic fluid confined in PS, a nanoscale single crystal material. We have evidenced the presence of capillary stresses during the freezing process probably due to the creation of liquid-vapour menisci introduced by contraction of the fluid during the phase transition. We could extract from our measurements both the amplitude of the strain (through the value of the porous layer lattice parameter) and the inhomogeneity of the strain (through the FWHM of the porous layer Bragg peak) during the freezing and melting of a confined alkane. Added to a previous DSC study of the thermal behaviour of the confined fluid [5], the present results allows a better understanding of the various thermodynamical process and of the strains involved in the freezing of an alkane confined in nanometer size pores.

The authors warmly thank A. Carminati and A. Delconte for their help to build the diffractometer, as well as during the X-ray diffraction experiments. We are very grateful to G.W. Scherer for fruitful discussions.

References

1. L.T. Canham, Appl. Phys. Lett. **57**, 1046 (1990).
2. in *Properties of porous silicon*, edited by L.T. Canham, (INSPEC, The Institution of Electrical Engineers, London, 1997).
3. D. Bellet, G. Dolino, Thin Solid Films **276**, 1 (1996); D. Bellet, G. Dolino in reference [2], p. 118.
4. R. Defay, I. Prigogine, *Tension superficielle et adsorption* (Maison Desser Editions, Liège, 1951); R. Defay, I. Prigogine, A. Bellemans, D.H. Everett, *Surface tension and adsorption* (Longmans, Green & Co, London, 1966).
5. C. Faivre, D. Bellet, G. Dolino, Euro. Phys. J. B **7**, 19 (1999).
6. P.J. Sereda, R.F. Feldman, in *Solid gas interfaces*, edited by E.A. Flood (Marcel Dekker, New York, 1967), Vol. 2, p. 729.
7. G.G. Litvan, Adv. Colloid Interface Sci. **9**, 253 (1978).
8. D. Bellet, G. Dolino, Phys. Rev. B **50**, 17162 (1994).
9. G. Dolino, D. Bellet, C. Faivre, Phys. Rev. B **54**, 17919 (1996).
10. C. Faivre, D. Bellet, G. Dolino, J. Appl. Phys. **87**, 2131 (2000).
11. V. Holy, U. Pietsch, T. Baumbach, *High-Resolution X-ray Scattering from Thin Films and Multilayers, Springer Tracts in modern Physics* (Springer-Verlag, Berlin, 1999), vol. 149.
12. K. Barla, G. Bomchil, R. Hérino, J.C. Pfister, A. Freund, J. Cryst. Growth **68**, 727 (1984).
13. D. Bellet, P. Lamagnère, A. Vincent, Y. Bréchet, J. Appl. Phys. **80**, 3772 (1996).
14. S.J. Greg, K.S.V. Singh, *Adsorption, surface area and porosity* (Academic, New York, 1982).
15. R. Hérino, G. Bomchil, K. Barla, C. Bertrand, J.L. Ginoux, J. Electrochem. Soc. **134**, 1994 (1987).

16. M. Brun, A. Lallemand, J.F. Quinson, C. Eyraud, Thermoch. Acta **21**, 59 (1977).
17. F.T. Meehan, Proc. R. Soc. London, A **115**, 199 (1927).
18. C. Hodgson, R. McIntosh, Can. J. Chem. **38**, 958 (1960).
19. G.G. Litvan, R. McIntosh, Can. J. Chem. **41**, 3095 (1963).
20. A.A. Antoniou, J. Phys. Chem. **68**, 2754 (1964).
21. R.F. Feldman, Can. J. Chem. **48**, 287 (1970).
22. G.G. Litvan, J. Colloid Interface Sci. **38**, 75 (1972).
23. J.G. Dash, H. Fu, J.S. Wettlaufer, Rep. Prog. Phys. **58**, 115 (1995).
24. D.H. Everett, Trans. Faraday Soc. **57**, 1541 (1961).
25. B.V. Enüstün, H.S. Sentürk, O. Yurdakul, J. Colloid Interface Sci. **65**, 509 (1978).
26. D. Buttard, D. Bellet, G. Dolino, J. Appl. Phys. **79**, 8060 (1996).
27. D. Bellet, L.T. Canham, Adv. Mater. **10**, 487 (1998).
28. G. Amato, N. Brunetto, A. Parisini, Thin Solid Films **297**, 73 (1997).
29. G. Scherer, J. Non-Cryst. Solids **155**, 1 (1993).